Effect of defocusing on picosecond laser-coupling into gold cones

I. A. Bush, A. G. R. Thomas, L. Gartside, S. Sarfraz, E. Wagenaars, J. S. Green, M. Notley, H. Lowe, C. Spindloe, T. Winstone, A. P. L. Robinson, R. Clarke, T. Ma, T. Yabuuchi, M. Wei, F. N. Beg, R. B. Stephens, A. MacPhee, A. J. MacKinnon, M. H. Key, W. Nazarov, M. Sherlock, and J. Pasley

Citation: Physics of Plasmas (1994-present) **21**, 012702 (2014); doi: 10.1063/1.4861375
View online: http://dx.doi.org/10.1063/1.4861375
View Table of Contents: http://scitation.aip.org/content/aip/journal/pop/21/1?ver=pdfcov
Published by the AIP Publishing

Effect of defocusing on picosecond laser-coupling into gold cones

I. A. Bush,[1,2,a)] A. G. R. Thomas,[3] L. Gartside,[1] S. Sarfraz,[1] E. Wagenaars,[1] J. S. Green,[2] M. Notley,[2] H. Lowe,[2] C. Spindloe,[2] T. Winstone,[2] A. P. L. Robinson,[2] R. Clarke,[2] T. Ma,[4] T. Yabuuchi,[4] M. Wei,[4] F. N. Beg,[4] R. B. Stephens,[5] A. MacPhee,[6] A. J. MacKinnon,[6] M. H. Key,[6] W. Nazarov,[7] M. Sherlock,[8] and J. Pasley[1,2]

[1]*York Plasma Institute, Department of Physics, University of York, York YO10 5DQ, United Kingdom*
[2]*Central Laser Facility, Rutherford Appleton Laboratory, Chilton OX11 0QX, United Kingdom*
[3]*Center for Ultrafast Optical Science, Nuclear Engineering and Radiological Sciences, University of Michigan, Ann Arbor, Michigan 48109-2099, USA*
[4]*Department of Mechanical and Aerospace Engineering, University of California San Diego, La Jolla, California 92093-0411, USA*
[5]*General Atomics, San Diego, California 92121-1122, USA*
[6]*Lawrence Livermore National Laboratory, Livermore, California 94550-9234, USA*
[7]*University of St. Andrews, School of Chemistry, St. Andrews KY16 9AJ, United Kingdom*
[8]*Blackett Laboratory, Imperial College of Science Technology and Medicine, London SW7 2AZ, United Kingdom*

(Received 17 October 2013; accepted 19 December 2013; published online 13 January 2014)

Here, we show that defocusing of the laser in the interaction of a picosecond duration, 1.053 μm wavelength, high energy pulse with a cone-wire target does not significantly affect the laser energy coupling efficiency, but does result in a drop in the fast electron effective temperature. This may be beneficial for fast ignition, since not only were more electrons with lower energies seen in the experiment but also the lower prepulse intensity will reduce the amount of preplasma present on arrival of the main pulse, reducing the distance the hot electrons have to travel. We used the Vulcan Petawatt Laser at the Rutherford Appleton Laboratory and gold cone targets with approximately 1 mm long, 40 μm diameter copper wires attached to their tip. Diagnostics included a quartz crystal imager, a pair of highly oriented pyrolytic graphite crystal spectrometers and a calibrated CCD operating in the single photon counting regime, all of which looked at the copper K_α emission from the wire. A short pulse optical probe, delayed 400 ps relative to the main pulse was employed to diagnose the extent of plasma expansion around the wire. A ray-tracing code modeled the change in intensity on the interior surface of the cone with laser defocusing. Using a model for the wire copper K_α emission coupled to a hybrid Vlasov-Fokker-Planck code, we ran a series of simulations, holding the total energy in electrons constant whilst varying the electron temperature, which support the experimental conclusions. [http://dx.doi.org/10.1063/1.4861375]

I. INTRODUCTION

Fast Ignition (FI)[1] is a variant upon the inertial confinement fusion (ICF)[2,3] scheme in which the hotspot is heated rapidly, out of pressure equilibrium with the surrounding fuel, in a manner that is independent of the compression process. One approach to achieving this is to expose the imploded dense fuel to an intense flux of ~MeV electrons, generated by a ~5 PW, 10–20 ps laser pulse. In order that the electrons couple effectively to the dense fuel, it is important that the region in which the laser accelerates the electrons be situated as close as possible to the fuel. One approach to achieving this is to embed a gold cone into the side of the capsule which contains the fusion fuel, such that the implosion compresses the fuel to a point just forward of the tip of the cone, on the cone axis.[4] This avoids the ignitor laser having to propagate through the large quantity of plasma pre-ablated by the longer pulse compression beams that would, in the absence of the cone, surround the imploded fuel mass. Initial experiments showed promising results,[5,6] however, these were conducted in a regime far removed from that in which ignition would be expected to occur.

A particular issue for fast ignition is that in order for efficient ignition to occur, the hotspot should be as compact as possible, while still meeting the areal density (ρr) conditions for ignition.[3] In order for the hotspot to ignite in fuel at densities of ~100 g cm^{-3}, when raised to a temperature of approximately 12 keV, it must have a ρr of approximately 0.5–0.6 g cm^{-2}. The bulk of the fuel must have a ρr on the order of 2–5 g cm^{-2} if a high fuel burn fraction is required. However, the bulk of this fuel should be heated only by the propagating burn wave once the hotspot has ignited. If the energy of the ignitor laser is dispersed over too large a volume of fuel, then an excessive laser energy will be required to raise the fuel to the ignition temperature (~12 keV). Forming a compact hotspot with laser generated electrons is challenging. In fast ignition, since the hotspot is formed out of pressure equilibrium with the surrounding fuel, it tends to disassemble rapidly. This limits the time available for

a)Electronic mail: ian.bush@gmail.com

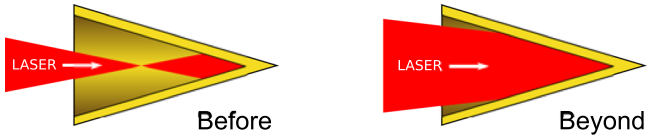

FIG. 1. Focusing the laser before the cone tip and beyond the cone tip.

heating the hotspot to 10–20 ps. Given the heat capacity of the hotspot, this implies that the heat flux must be very high; approaching $10^{20}\,\mathrm{W\,cm^{-2}}$. Given coupling inefficiencies between the laser and the hot electrons that reach the dense fuel, this means that the heating laser intensity must be of the order $10^{21}\,\mathrm{W\,cm^{-2}}$. Existing high-power, high-energy laser systems are built with neodymium doped glass laser amplifiers, which operate at a wavelength of 1.053 μm. At this wavelength, and at intensities on the order $10^{21}\,\mathrm{W\,cm^{-2}}$, laser-plasma interactions generate an electron distribution with a characteristic temperature above 1 MeV.[7,8] This means there will be a significant fraction of the energy in electrons which have a range in the dense fuel that is much greater than $0.5\,\mathrm{g\,cm^{-2}}$.[1] Therefore, there are conflicting requirements placed upon the laser system. An obvious approach to solving this problem is to operate at shorter laser wavelengths, by means of non-linear optical frequency doubling techniques. This solution is not ideal, however, since a significant fraction of the energy in the laser beam would be lost in the process of reducing the wavelength. Here, we discuss a technique which appears to soften the electron spectrum entering a target, whilst maintaining the overall energy coupled to the energetic electron population.

Another issue that is of relevance to the present study is that of laser prepulse interaction with the cone, which forms plasma. This prepulse, which is of approximately nanosecond duration, comes predominantly from amplified spontaneous emission (ASE) and can contain 10^{-4} of the energy of the main pulse. This plasma can obstruct the propagation of the high intensity portion of the laser pulse, and therefore shift the site of relativistic electron production away from where the fuel would be located in the fast ignition case. Recent experiments have looked to characterise this preplasma and have observed $\sim$100 μm depth of plasma filling in a cone-like target.[9]

A recent experiment performed using the Titan Laser facility at Lawrence Livermore National Laboratory's Jupiter Laser Facility showed an unexpected result when a high energy picosecond laser pulse was focused past the tip of a copper cone. An increase in signal was shown on a thermoluminescent detector, which is sensitive to γ and β radiation, compared to the case when the laser was focused tightly onto the interior of the cone tip.[10,11] The results presented here are from a recent experiment on the Vulcan Petawatt laser, at the Rutherford Appleton Laboratory, carried out in part to further investigate the behavior of laser cone-coupling in cases where the laser is not focused tightly upon the interior of the cone tip. The effect of defocusing upon laser coupling into copper wires mounted on the tips of gold cones is investigated. The laser is focused either before, beyond, or at the interior surface of the cone tip, as shown in Figure 1.

II. EXPERIMENTAL SETUP

The Vulcan Petawatt laser is a neodymium doped glass laser, with a wavelength of 1.053 μm, which employs chirped pulsed amplification to obtain PW power and focused intensities of up to around $2 \times 10^{21}\,\mathrm{W\,cm^{-2}}$. The energies of the laser pulses employed in this experiment were 600 ± 100 J with a pulse duration of 1 ± 0.5 ps. The laser was focused using an *f*/3 off-axis parabolic mirror, resulting in a spot size of 8 μm (FWHM) and a peak intensity of $\sim 10^{21}\,\mathrm{W\,cm^{-2}}$. Measurements made during the experiment showed that the prepulse has an intensity contrast of approximately 10^{-7}, with the pedestal extending for $\sim$1 ns before the main pulse, equating to an energy contrast of around 10^{-4}. The prepulse has the same spatial distribution as the main pulse.

The cones employed in the experiment, shown in Figure 2, were 1.5 mm in length, with a half angle of 20°, and 20 μm thick walls. The tip of the cone was 30 μm in diameter with a thickness of 6 μm. To measure the energy coupling into the regions forward of the cone tip, copper wires approximately 1 mm long and 40 μm in diameter were glued onto the tip of the cone. By using copper K_α diagnostics to look at the X-ray emission from the wire attached to the tip, information about the total energy and energy spectrum of the hot electrons produced by the laser-solid interaction can be obtained.[12,13]

An electron spectrometer was also used in the experiment, however, whilst the spectra measured by this diagnostic support the trends inferred from the 1/*e* length analysis, they cannot be analysed in such a way as to provide a meaningful quantitative picture of the electron population within the target. This is due to electric fields that are created within and around the target as electrons escape.[12,13] Low energy electrons are less likely to escape the target, and higher energy particles are decelerated in escaping the sheath field.

A Bragg reflecting crystal was used to image the emission from the wires. The crystal was quartz SiO_2 2131, providing a magnification of 8×. The Bragg angle was 88.7° for 8 keV X-rays, with the image being recorded on to Fujifilm BAS-SR image plates.[14]

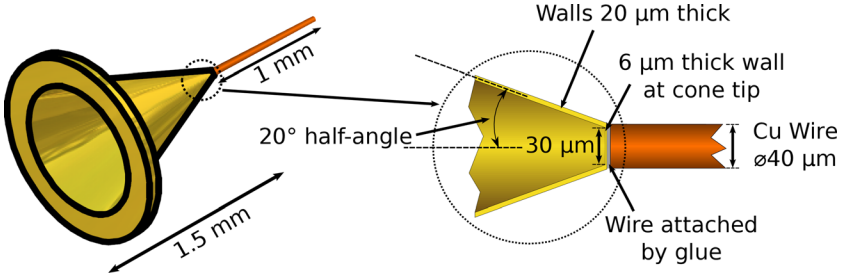

FIG. 2. Diagram of cone-wire targets, showing an enlarged version of the cone-tip.

A pair of highly oriented pyrolytic graphite (HOPG) spectrometers were employed; working in third order, both could resolve copper $K_{\alpha 1}$ at 8047 eV and copper $K_{\alpha 2}$ at 8027 eV. They were based upon mosaic Bragg reflecting crystals, with a mosaic spread of $0.4 \pm 0.1^{\circ}$ (ZYA).[15] The spectrum was also recorded onto Fujifilm BAS-SR image plates. Both spectrometers were positioned above the target and perpendicular to one another.

A single hit charge coupled device (SHCCD) was also used to measure total K_{α} yields. Copper foils were shot during the experiment to cross-calibrate the SHCCD with the HOPG spectrometers.

An electron spectrometer was used, aligned such that it was looking straight down the axis of the cone-wire targets. A 2ω optical probe was used with channels for interferometry and shadowgraphy, delayed to 400 ps after the main pulse. The shadowgraphy imagery was used to diagnose the extent of the plasma expansion around the wire.

III. RESULTS AND ANALYSIS

Figure 3(a) shows a typical image plate scan and line-out from the copper K_{α} imager. The line-out shows an exponential fall off of copper K_{α} emission along the wire. In many shots, a brightening again at the far end of the wire is seen, which is likely due to refluxing in the target of a high energy component of the electron spectrum.[16] This part of the spectrum, which makes a negligible difference in the first 250 μm of the wire, is not considered in this analysis; it has been observed in a number of previous experiments.[17] The low temperature component of the spectrum, with electron energies of a few MeV, is most important for FI applications. The experimental result is shown alongside a simulation result from the 2D hybrid Vlasov-Fokker-Planck code, FIDO.[18] K_{α} photon density production was calculated using relativistic binary-encounter cross sections[19] directly from the hot electron distribution function.[20] The electron beam was injected into a domain of 40 μm $\times$ 250 μm with reflecting boundary conditions representing the wire edge, and an open boundary at 250 μm. Wilk's scaling[21] was used to relate the fast electron effective temperature to the intensity. The defocus position was determined from the ray-tracing code, detailed below. These results were convolved with a Gaussian instrument function with a standard deviation of 35 ± 10 μm, to account for the experimental resolution of the K_{α} imager.

The Bragg reflecting crystal used to image the wires has a very narrow bandwidth, 6 eV in this experimental setup, and the copper K_{α} line shifts and broadens at higher temperatures.[22] A correction has to be made to account for this; to infer the temperature at different points along the wire modelling was performed in the 1D radiation hydrodynamics code HYADES.[23] The expansion of the wire from HYADES was then compared to the expansion of the cut-off density surface, at 5×10^{19} cm^{-3}, seen by the optical probe (Figure 3(b)). This cut-off density takes into account the finite size of the imaging optics and refraction in the plasma, an identical setup was used previously by Lancaster *et al.*[24] A correction for the inferred temperature shift along the wire was then made using a similar methodology to Ref. 22. The correction factor ranges from a 3.5$\times$ increase in the hottest part of the wire, down to a 1.5$\times$ increase in the coolest part, as shown in Figure 3(a).

In Figure 4(a), the variation of copper K_{α} yield, from the first 250 μm in the wire, against the defocus distance is shown. Total copper K_{α} yields were determined by calibration of the HOPG spectrometers via the SHCCD. To obtain

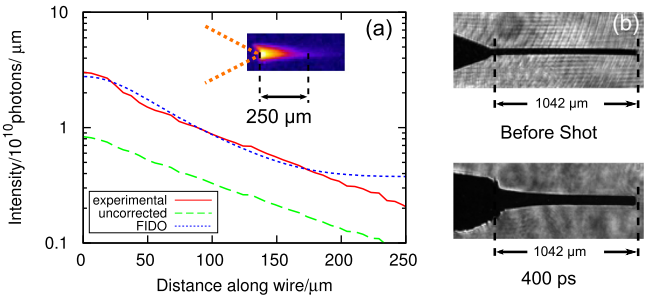

FIG. 3. (a) Image plate scan and line-out from K_{α} imager, alongside the line-out without correcting for the frequency shift on the imager, and a normalised FIDO simulation result. (b) Probe image before the shot and at 400 ps after the shot. Both (a) and (b) are for the same shot, where the laser was focused 800 μm before the cone tip.

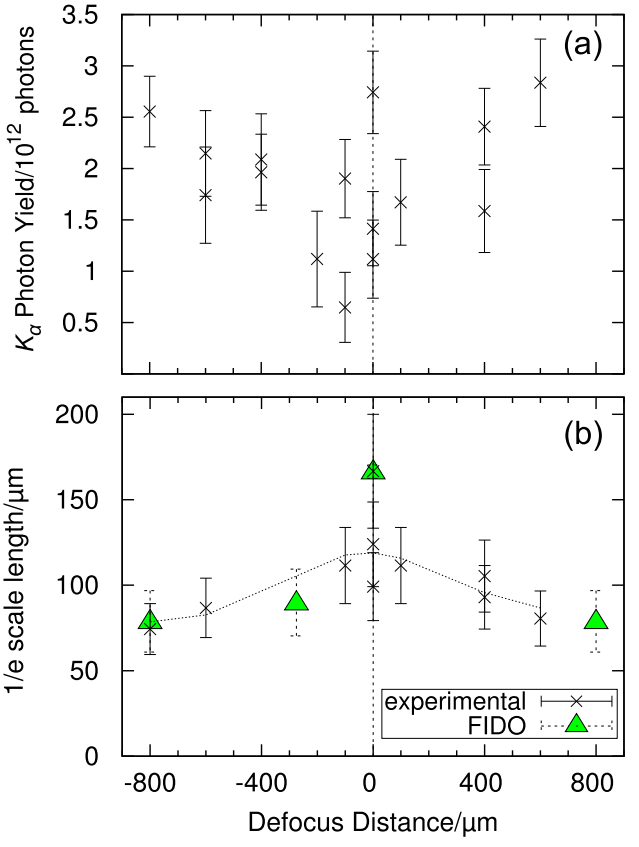

FIG. 4. (a) Variation of copper K_{α} yield in first 250 μm in the wire with focus position. The error bars show the uncertainty when comparing shots, the error from the calibration is larger. The negative values on the x-axis indicate a focus before the cone tip and positive values a laser focus beyond the cone tip (Figure 1). (b) Variation of length over which K_{α} emission falls to $1/e$ of its peak value with defocus distance. The dotted lines show a weighted moving average across ± 400 μm. The FIDO simulation results are shown after taking a convolution with a Gaussian instrument function with a standard deviation of 35 ± 10 μm.

just the yield in the first 250 μm of wire, a correction was applied from the spatial information obtained by the K_α imager. The errors on the graph indicate the uncertainty between different shots in the yield from the HOPG spectrometers. The systematic calibration error is larger, estimated to be $\pm 50\%$. In addition, there is shot to shot variation, this is due to factors such as alignment of the targets, changes in the laser pulse, and differences between the targets. The total K_α yield is shown to weakly increase with increasing electron temperature, for a fixed laser pulse energy, in simulations performed using FIDO. Approximating a cylindrical system from the Cartesian distribution, the total K_α photon yield from the FIDO simulations ranged from 10.4×10^{12} photons at an intensity of 0.1×10^{21} W cm^{-2} up to 17.0×10^{12} photons at 1×10^{21} W cm^{-2}, which is only a 1.7× variation in yield for an order of magnitude change in intensity. The FIDO results show that a weak increase would be expected in K_α photon yield for the tight focus case. Hence, the energy coupling, inferred from the K_α photon yield shown in Figure 4, does not change significantly with defocus.

Figure 4(b) shows the variation in the length along the wire over which the copper K_α emission falls to $1/e$ of its original value. Also shown are results from FIDO simulations, at intensities of 0.1, 0.3, and 1×10^{21} W cm^{-2}. These were performed by varying the spot size, while keeping the total electron energy constant, corresponding to ± 800 μm, -275 μm, and tight focus, respectively. The FIDO simulations show that the $1/e$ scale length becomes longer for higher energy electron distributions, as the electrons will travel further before being slowed by collisional and resistive stopping. The same result is seen in the experiment, with the longest electron scale length corresponding to a shot at tight focus. With higher levels of defocus, the electron scale length drops by a factor of ~2, in both the experiment and simulations. The fact the scale length varies most close to tight focus may explain the scatter in the scale length results at 0 μm. The results in Figure 4 are expected, on the basis of previous studies which show the variation of hot electron temperature in a laser-solid target interaction as function of laser intensity.[21,25]

The details of the absorption are complex, and the exact scaling of the hot electron spectrum with laser intensity is likely to be significantly more involved than in the model used here. However, it is reasonable to assume that the highest effective temperature for the fast electrons would be expected from tight focus, which is also supported by the experimental diagnostics. Hence, although the injection model for fast electrons into the FIDO simulation may be insufficient to describe the details of the interaction, the general trend is expected to be correct.

IV. RAY-TRACING

A ray-tracing code was created in order to look at the intensity variation across the inside of the cone when the laser is defocused. The code follows a similar method to that described in Ref. 26, but calculates analytically the intersections and reflections in three dimensions. Reflectivity and absorption from both the cone walls and the tip are calculated using a fixed absorption model, as described in Ref. 10. Although this is based on data from the Jupiter Laser Facility, similar absorption has been observed on an experiment at the Vulcan Petawatt laser.[17] At the parabolic mirror, which is 650 mm in diameter, the FWHM of the laser beam is 600 mm (slightly more in the vertical direction) and the focal spot has an 8 μm FWHM. The total laser power is taken to be 1 PW. No interference effects were taken into account in the code.

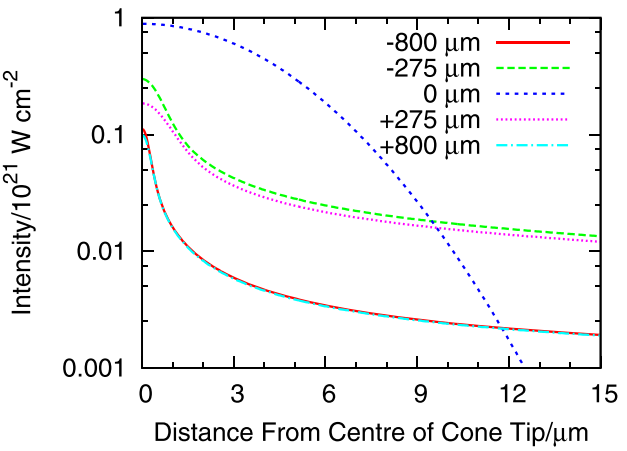

FIG. 5. Intensity across the flat cone tip, as shown in Figure 2. Results are for tight focus (0 μm), ± 275 μm, and ± 800 μm.

Figure 5 shows the intensity across the cone tip. For the ± 275 μm defocused cases, the peak intensities are ~100× higher than when reflections are turned off in the ray-tracing code. This suggests that the cone is acting as an efficient light guide for the laser energy.

Reduced prepulse intensities will result in a substantial reduction in preplasma formation at the cone tip.[9] It is possible therefore that, although the laser intensity at the tip is lower, more energy reaches the wire since the point of laser absorption is now moved closer to the cone tip. For the tight focus case, it is expected that the preplasma will increase the total laser energy absorption in the target,[27] but fewer of the hot electrons in this case will enter the copper wire.

V. DISCUSSION AND SUMMARY

From the data collected in the experiment, it appears that defocusing the laser maintains the overall energy coupled into the cone, but softens the spectrum of the generated electrons, for the low temperature component of the electron spectrum. An ability to have some control of this part of the electron spectrum, without a large drop in laser-energy coupling, could be useful in fast ignition by virtue of permitting the creation of a more compact hotspot. In this experiment, the copper wire acts to stop the electron beam spreading too far; however, in a real fast ignition target, the geometry is more complicated, and the defocusing could have the disadvantage of increasing the source diameter of the beam of the fast electrons. This might limit the usefulness of such a technique, so the net effect on a fast ignition scheme still requires further investigation.

Care must be taken in extrapolating these results to a full scale re-entrant cone guided fast ignition scheme. Although there are a number of technologies that are presently being explored to increase laser contrast, the substantially higher laser energy that would be employed in fast ignition fusion experiments might well still have a higher level of prepulse associated with it than that which was present here. While we would anticipate a softening of the electron spectrum in this case, the integrity of the cone surface may be compromised sooner in the case of a higher energy prepulse, resulting in a reduction in coupling.

ACKNOWLEDGMENTS

This work was supported in part by DTRA under Basic Research Award No. HDTRA1-10-10077.

[1]M. Tabak, J. Hammer, M. E. Glinsky, W. L. Kruer, S. C. Wilks, J. Woodworth, E. M. Campbell, M. D. Perry, and R. J. Mason, Phys. Plasmas **1**, 1626 (1994).
[2]J. Nuckolls, L. Wood, A. Thiessen, and G. Zimmerman, Nature **239**, 139 (1972).
[3]J. Lindl, Phys. Plasmas **2**, 3933 (1995).
[4]M. Tabak, J. H. Hammer, E. M. Campbell, W. L. Kruer, J. Goodworth, S. C. Wilks, and M. Perry, Lawrence Livermore National Laboratory patent disclosure IL8826B (1997).
[5]R. Kodama, P. A. Norreys, K. Mima, A. E. Dangor, R. G. Evans, H. Fujita, Y. Kitagawa, K. Krushelnick, T. Miyakoshi, N. Miyanaga, T. Norimatsu, S. J. Rose, T. Shozaki, K. Shigemori, A. Sunahara, M. Tampo, K. A. Tanaka, Y. Toyama, T. Yamanaka, and M. Zepf, Nature **412**, 798 (2001).
[6]P. A. Norreys, K. L. Lancaster, C. D. Murphy, H. Habara, S. Karsch, R. J. Clarke, J. Collier, R. Heathcote, C. Hemandez-Gomez, S. Hawkes, D. Neely, M. H. R. Hutchinson, R. G. Evans, M. Borghesi, L. Romagnani, M. Zepf, K. Akli, J. A. King, B. Zhang, R. R. Freeman, A. J. MacKinnon, S. P. Hatchett, P. Patel, R. Snavely, M. H. Key, A. Nikroo, R. Stephens, C. Stoeckl, K. A. Tanaka, T. Norimatsu, Y. Toyama, and R. Kodama, Phys. Plasmas **11**, 2746 (2004).
[7]H. Chen, S. C. Wilks, W. L. Kruer, P. K. Patel, and R. Shepherd, Phys. Plasmas **16**, 020705 (2009).
[8]T. Tanimoto, H. Habara, R. Kodama, M. Nakatsutsumi, K. A. Tanaka, K. L. Lancaster, J. S. Green, R. H. H. Scott, M. Sherlock, P. A. Norreys, R. G. Evans, M. G. Haines, S. Kar, M. Zepf, J. King, T. Ma, M. S. Wei, T. Yabuuchi, F. N. Beg, M. H. Key, P. Nilson, R. B. Stephens, H. Azechi, K. Nagai, T. Norimatsu, K. Takeda, J. Valente, and J. R. Davies, Phys. Plasmas **16**, 062703 (2009).
[9]S. D. Baton, M. Koenig, J. Fuchs, A. Benuzzi-Mounaix, P. Guillou, B. Loupias, T. Vinci, L. Gremillet, C. Rousseaux, M. Drouin, E. Lefebvre, F. Dorchies, C. Fourment, J. J. Santos, D. Batani, A. Morace, R. Redaelli, M. Nakatsutsumi, R. Kodama, A. Nishida, N. Ozaki, T. Norimatsu, Y. Aglitskiy, S. Atzeni, and A. Schiavi, Phys. Plasmas **15**, 042706 (2008).
[10]L. van Woerkom, K. U. Akli, T. Bartal, F. N. Beg, S. Chawla, C. D. Chen, E. Chowdhury, R. R. Freeman, D. Hey, M. H. Key, J. A. King, A. Link, T. Ma, A. J. MacKinnon, A. G. MacPhee, D. Offermann, V. Ovchinnikov, P. K. Patel, D. W. Schumacher, R. B. Stephens, and Y. Y. Tsui, Phys. Plasmas **15**, 056304 (2008).
[11]R. J. Clarke, D. Neely, R. D. Edwards, P. N. M. Wright, K. W. D. Ledingham, R. Heathcote, P. McKenna, C. N. Danson, P. A. Brummitt, J. L. Collier, P. E. Hatton, S. J. Hawkes, C. Hernandez-Gomez, P. Holligan, M. H. R. Hutchinson, A. K. Kidd, W. J. Lester, D. R. Neville, P. A. Norreys, D. A. Pepler, T. B. Winstone, R. W. W. Wyatt, and B. E. Wyborn, J. Radiol. Prot. **26**, 277 (2006).
[12]R. Kodama, Y. Sentoku, Z. L. Chen, G. R. Kumar, S. P. Hatchett, Y. Toyama, T. E. Cowan, R. R. Freeman, J. Fuchs, Y. Izawa, M. H. Key, Y. Kitagawa, K. Kondo, T. Matsuoka, H. Nakamura, M. Nakatsutsumi, P. A. Norreys, T. Norimatsu, R. A. Snavely, R. B. Stephens, M. Tampo, K. A. Tanaka, and T. Yabuuchi, Nature **432**, 1005 (2004).
[13]J. A. King, K. U. Akli, R. R. Freeman, J. Green, S. P. Hatchett, D. Hey, P. Jamangi, M. H. Key, J. Koch, K. L. Lancaster, T. Ma, A. J. MacKinnon, A. Macphee, P. A. Norreys, P. K. Patel, T. Phillips, R. B. Stephens, W. Theobald, R. P. J. Town, L. van Woerkom, B. Zhang, and F. N. Beg, Phys. Plasmas **16**, 020701 (2009).
[14]K. A. Tanaka, T. Yabuuchi, T. Sato, R. Kodama, Y. Kitagawa, T. Takahashi, T. Ikeda, Y. Honda, and S. Okuda, Rev. Sci. Instrum. **76**, 013507 (2005).
[15]A. Pak, G. Gregori, J. Knight, K. Campbell, D. Price, B. Hammel, O. L. Landen, and S. H. Glenzer, Rev. Sci. Instrum. **75**, 3747 (2004).
[16]T. Ma, H. Sawada, P. K. Patel, C. D. Chen, L. Divol, D. P. Higginson, A. J. Kemp, M. H. Key, D. J. Larson, S. Le Pape, A. Link, A. G. MacPhee, H. S. McLean, Y. Ping, R. B. Stephens, S. C. Wilks, and F. N. Beg, Phys. Rev. Lett. **108**, 115004 (2012).
[17]M. Nakatsutsumi, J. R. Davies, R. Kodama, J. S. Green, K. L. Lancaster, K. U. Akli, F. N. Beg, S. N. Chen, D. Clark, R. R. Freeman, C. D. Gregory, H. Habara, R. Heathcote, D. S. Hey, K. Highbarger, P. Jaanimagi, M. H. Key, K. Krushelnick, T. Ma, A. MacPhee, A. J. MacKinnon, H. Nakamura, R. B. Stephens, M. Storm, M. Tampo, W. Theobald, L. V. Woerkom, R. L. Weber, M. S. Wei, N. C. Woolsey, and P. A. Norreys, New J. Phys. **10**, 043046 (2008).
[18]M. Sherlock, Phys. Plasmas **16**, 103101 (2009).
[19]J. P. Santos, F. Parente, and Y.-K. Kim, J. Phys. B: At. Mol. Phys. **36**, 4211 (2003).
[20]A. G. R. Thomas, M. Sherlock, C. Kuranz, C. P. Ridgers, and R. P. Drake, New J. Phys. **15**, 015017 (2013).
[21]S. C. Wilks and W. L. Kruer, IEEE J. Quantum Electron. **33**, 1954 (1997).
[22]K. U. Akli, M. H. Key, H. K. Chung, S. B. Hansen, R. R. Freeman, M. H. Chen, G. Gregori, S. Hatchett, D. Hey, N. Izumi, J. King, J. Kuba, P. Norreys, A. J. MacKinnon, C. D. Murphy, R. Snavely, R. B. Stephens, C. Stoeckel, W. Theobald, and B. Zhang, Phys. Plasmas **14**, 023102 (2007).
[23]J. T. Larsen and S. M. Lane, J. Quantum Spectrosc. Radiat. Transfer **51**, 179 (1994).
[24]K. L. Lancaster, J. Pasley, J. S. Green, D. Batani, S. Baton, R. G. Evans, L. Gizzi, R. Heathcote, C. Hernandez Gomez, M. Koenig, P. Koester, A. Morace, I. Musgrave, P. A. Norreys, F. Perez, J. N. Waugh, and N. C. Woolsey, Phys. Plasmas **16**, 056707 (2009).
[25]F. N. Beg, A. R. Bell, A. E. Dangor, C. N. Danson, A. P. Fews, M. E. Glinsky, B. A. Hammel, P. Lee, P. A. Norreys, and M. Tatarakis, Phys. Plasmas **4**, 447 (1997).
[26]G. Rinker and G. Bohannon, IEEE Trans. Plasma Sci. **8**, 55 (1980).
[27]Y. Ping, R. Shepherd, B. F. Lasinski, M. Tabak, H. Chen, H. K. Chung, K. B. Fournier, S. B. Hansen, A. Kemp, D. A. Liedahl, K. Widmann, S. C. Wilks, W. Rozmus, and M. Sherlock, Phys. Rev. Lett. **100**, 085004 (2008).